

# Surface diffusion of *n*-alkanes: Mechanism and anomalous behavior

Jae Hyun Park, N.R. Aluru \*

*Beckman Institute for Advanced Science and Technology, University of Illinois at Urbana-Champaign, Urbana, IL 61801, United States*

Received 16 August 2007; in final form 16 September 2007

Available online 21 September 2007

## Abstract

In this Letter, we investigate, using molecular dynamics simulations, the diffusion of *n*-octane and *n*-tetradecane on a graphite surface at 300 K under incomplete coverage condition. For both molecules, we observe that the lateral diffusion coefficient exhibits a  $\Lambda$ -shape anomaly with surface coverage i.e., the diffusion coefficient increases with the increase in surface coverage until a critical surface coverage, beyond which the diffusion coefficient decreases. Moreover, for low surface coverages, the longer *n*-tetradecane molecule moves faster compared to the shorter *n*-octane molecule and for high surface coverages, the *n*-octane molecule moves faster. We develop a new theory to understand the surface diffusion of *n*-alkanes and show that  $D \sim \frac{r_{se}^2}{N^p \epsilon_R}$ .

© 2007 Elsevier B.V. All rights reserved.

## 1. Introduction

Diffusion of liquids on solid substrates has been a focus of significant interest for many years not only because of the numerous applications that rely on this physical phenomena (e.g. nanotribology and wetting/dewetting of complex and functional surfaces [1,2]) but also because of its scientific importance [3]. The emerging area of nanofluidic sciences, where the concentration of the sample can be significantly smaller, requires a detailed understanding of the surface diffusion of liquids when the surface coverage is less than a monolayer (referred to as incomplete coverage) [4]. When the surface is incompletely covered, the molecular motion of the liquid can be dramatically different from its bulk counterpart. For example, Zhao and Granick [5,6] observed that the surface diffusion of long polyethylene glycol (PEG) chains exhibits a nonmonotonic dependence i.e., the surface diffusion increases with increasing surface concentration, and then decreases abruptly. However, the molecular mechanisms governing the surface diffusion are not clear [7]. In spite of their simple structure, *n*-alkanes can capture the essential features of complex and practical chains, and hence, have been used extensively to

investigate various properties of complex chains. Xia et al. [8] simulated *n*-hexadecane films adsorbed on a Au(001) surface using molecular dynamics and observed that the lateral diffusion is augmented significantly with the reduction in film thickness.

In this Letter, by performing extensive molecular dynamics simulations on the diffusion of *n*-alkanes as a function of surface coverage, we explain in detail the mechanism governing the surface diffusion of short and long chain molecules and, more interestingly, report for the first time that *n*-alkanes exhibit anomalous diffusion for low surface coverage.

## 2. Method

We have used molecular dynamics simulations to investigate the diffusion of *n*-alkanes on a graphite surface under incomplete coverage condition (see Fig. 1). Two typical *n*-alkanes – *n*-octane ( $n\text{-C}_8\text{H}_{18}$ ) and *n*-tetradecane ( $n\text{-C}_{14}\text{H}_{30}$ ) were considered. Both are short enough to ignore the entanglement effects [8]. An *n*-alkane molecule was modeled as an united atom (UA) chain [9], in which each methylene ( $\text{CH}_2$ ) and methyl ( $\text{CH}_3$ ) group is represented as a single interacting segment with different mass. Both bending and torsion were included with fixed bonding distance while each segment was modeled as Lennard-Jones (LJ)

\* Corresponding author. Fax: +1 217 244 4333.

E-mail address: [aluru@uiuc.edu](mailto:aluru@uiuc.edu) (N.R. Aluru).

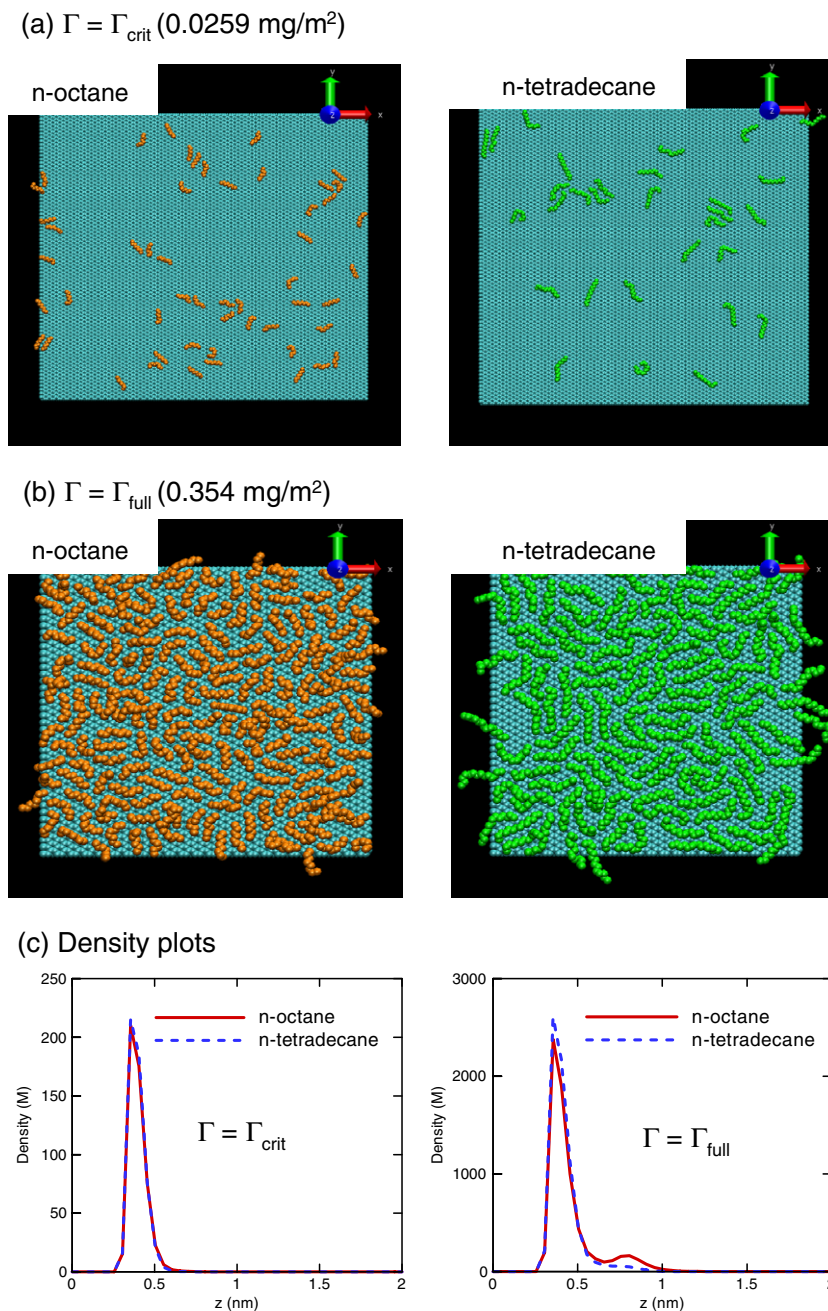


Fig. 1. Molecular visualization of *n*-alkane molecules on a graphite surface for incomplete surface coverage: (a)  $\Gamma = \Gamma_{\text{crit}}$ , the maximum diffusion is observed; (b)  $\Gamma = \Gamma_{\text{full}}$ , the surface is fully covered by *n*-alkane molecules; (c) density plots (*z*-axis is perpendicular to the plate). A second layer starts to form for  $\Gamma = \Gamma_{\text{full}}$ . The snapshot was rendered using VMD [20].

particles [9]. The LJ interaction was not considered for the segments which are connected by less than four bonds. The carbon atoms in the graphite surface were modeled as fro-

zen LJ particles [10]. The Lennard-Jones parameters are summarized in Table 1. The parameters for different kinds of segments/atoms were calculated by using the linear combination rule.

For each chain molecule, various surface coverages (denoted by  $\Gamma$ ) ranging from  $\Gamma = 4.97 \times 10^{-4}$  mg/m<sup>2</sup> to  $\Gamma = 0.355$  mg/m<sup>2</sup> were considered. The surface coverage was measured as the ratio of the total mass of the chain molecules to the graphite surface area. Table 2 summarizes the various cases considered in this study. The smallest surface coverage ( $4.97 \times 10^{-4}$  mg/m<sup>2</sup> for *n*-octane and

Table 1  
Lennard-Jones parameters

Pair	$\sigma$ (nm)	$\epsilon$ (kJ/mol)	Ref.
CH <sub>3</sub> –CH <sub>3</sub>	0.3930	0.9478	[9]
CH <sub>2</sub> –CH <sub>2</sub>	0.3930	0.4148	[9]
C–C	0.3390	0.2897	[10]

Table 2  
Surface coverage conditions considered in this study

<i>n</i> -Octane		<i>n</i> -Tetradecane	
#. mols.	$\Gamma$ (mg/m <sup>2</sup> )	#. mols.	$\Gamma$ (mg/m <sup>2</sup> )
1	$4.97 \times 10^{-4}$	1	$8.64 \times 10^{-4}$
8	$3.98 \times 10^{-3}$	5	$4.32 \times 10^{-3}$
13	$6.47 \times 10^{-3}$	8	$6.91 \times 10^{-3}$
26	0.0129	15	0.0130
52	0.0259	30	0.0259
139	0.0691	80	0.0691
278	0.138	160	0.138
156 <sup>a</sup>	0.288	89 <sup>a</sup>	0.288
192 <sup>a</sup>	0.354	111 <sup>a</sup>	0.355

The area of graphite surface in MD simulations is  $A = 381.38 \text{ nm}^2$  except for the two highest surface coverage cases.

<sup>a</sup> Graphite surface area  $A = 102.91 \text{ nm}^2$ .

$8.64 \times 10^{-4} \text{ mg/m}^2$  for *n*-tetradecane) corresponds to the case of a single molecule on the graphite surface. For both *n*-alkanes, the graphite surface is completely covered for  $\Gamma_{\text{full}} = 0.355 \text{ mg/m}^2$ . Beyond this coverage, a second layer starts to form (see Fig. 1c).

Simulations were performed using modified GROMACS 3.2.1 [11] in an NVT ensemble. The graphite surface consists of three graphene layers and its dimension was  $19.88 \text{ nm} \times 19.184 \text{ nm}$  (*xy*-plane) when  $\Gamma$  is less than  $0.014 \text{ mg/m}^2$  and  $10.082 \text{ nm} \times 10.207 \text{ nm}$  for the cases where  $\Gamma$  is larger than  $0.014 \text{ mg/m}^2$ . A purely reflecting wall was located far from the first graphene layer (at  $z = 40.0 \text{ nm}$ ) to prevent the escape of molecules. Periodic boundary conditions were assigned along *x*- and *y*-directions. In the *z*-direction, an extra empty space of  $10 \text{ nm}$  was placed on top of the reflecting wall to eliminate interaction between replicated images. All simulations were equilibrated for  $2 \text{ ns}$ . The sampling period was  $10 \text{ ns}$ . The LINCS algorithm [12] was used to maintain the molecular shape of *n*-alkanes. The Nosé-Hoover thermostat [13,14] with time constant of  $1.0 \text{ ps}$  was used to maintain the system temperature at  $300 \text{ K}$ . The equation of motion was integrated by using the leapfrog algorithm with a time step of  $2.0 \text{ fs}$ .

### 3. Results and discussion

Fig. 2 shows the lateral diffusion coefficient for various surface coverages. Diffusion of the liquid perpendicular to the solid surface (*z*-direction) is negligible ( $D_{\perp} \sim 10^{-12} \text{ m}^2/\text{s}$ ), so we do not investigate it any further in this Letter. Lateral diffusion coefficient was computed from the mean-squared displacement of the center-of-mass of the molecule, i.e.,

$$D = \lim_{t \rightarrow \infty} \frac{\langle |\mathbf{R}_{\text{CM}}(t) - \mathbf{R}_{\text{CM}}(0)|^2 \rangle}{4t} \quad (1)$$

where  $\mathbf{R}_{\text{CM}}$  is the (*x*,*y*)-position of the center-of-mass of the molecule. Throughout this Letter, the *diffusion* coefficient refers to the *lateral diffusion* coefficient unless specified,

otherwise. From the figure, we make two key observations: (1) regardless of the molecule type, the diffusion coefficient gradually increases with the decrease in surface coverage until it reaches a critical surface coverage ( $\Gamma_{\text{crit}} = 0.026 \text{ mg/m}^2$ ,  $\Gamma_{\text{crit}}/\Gamma_{\text{full}} = 0.073$ ) and then starts to decrease with a further decrease in the surface coverage (this is referred to as  $\Lambda$ -shape) (2) *n*-octane (shorter chain) moves faster for high surface coverages while *n*-tetradecane (longer chain) moves faster in the low coverage limit (see the inset in Fig. 2a). The fast diffusion of longer *n*-tetradecane compared to the shorter *n*-octane is a surprising anomalous behavior compared to the bulk case. From Fig. 2b, which shows the variation of the diffusion coefficient with the number of molecules, we can observe more clearly the fast diffusion of the longer *n*-alkane for fewer number of molecules on the surface. The maximum diffusion coefficient of the *n*-alkanes ( $1.125 \times 10^{-7} \text{ m}^2/\text{s}$  for *n*-octane and  $8.867 \times 10^{-8} \text{ m}^2/\text{s}$  for *n*-tetradecane) are over 30 times larger than their bulk values ( $3.36 \times 10^{-9} \text{ m}^2/\text{s}$  for *n*-octane and  $1.83 \times 10^{-9} \text{ m}^2/\text{s}$  for *n*-tetradecane). The *n*-octane diffusion coefficient for  $\Gamma = \Gamma_{\text{full}}$  is  $6.56 (\pm 0.04) \times 10^{-9} \text{ m}^2/\text{s}$ , which is about an order of magnitude higher than the reported value of  $D = 0.57 \times 10^{-9} \text{ m}^2/\text{s}$  for 1.3 monolayers coverage of liquid *n*-octane adsorbed on  $\alpha\text{-Al}_2\text{O}_3(0001)$  at  $300 \text{ K}$ . This is because  $\alpha\text{-Al}_2\text{O}_3(0001)$  has a stronger interaction with *n*-alkane [15].

Previous studies also reported the  $\Lambda$ -shape anomaly in surface diffusion of a flexible polymer (polyethylene glycol, PEG) using experiments [5,6] and MD simulations [7]. The maximum diffusion coefficient was observed to be at the onset of full coverage where the molecular conformation changes from *pancake* to *loop-train-tail*. However, in the present study the maximum diffusion coefficient was observed when the surface coverage was  $7.3\%$  ( $\Gamma_{\text{crit}}/\Gamma_{\text{full}} = 0.073$ ) regardless of the molecule type. This implies that the physical mechanism governing the  $\Lambda$ -shape anomaly could be different. Furthermore, the *loop-train-tail* conformation is not typically observed in *n*-alkanes due to their high rigidity. Considering the above results and discussion, in the rest of this letter we focus on two questions: (1) what is the molecular mechanism governing the  $\Lambda$ -shape anomaly of surface diffusion of *n*-alkanes? (2) why does the longer *n*-tetradecane move faster than the shorter *n*-octane for low surface coverage? To elucidate the physical mechanisms underlying these observations, we exploit the well-known relation between translational and rotational motion of chain molecules [16,17] for bulk systems and extend it to the surface diffusion case.

For a concentrated solution of rod-like molecules, the (global) rotational relaxation time of a molecule,  $\tau_R$ , is related to its translational diffusion coefficient,  $D_{\text{bulk}}$ , by the expression [16],

$$D_{\text{bulk}} \sim \frac{r_{\text{ee}}^2}{\tau_R}, \quad (2)$$

where  $r_{\text{ee}}$  is the end-to-end distance of the molecule and by approximating *n*-alkanes as Rouse chains,  $\tau_R$  is computed

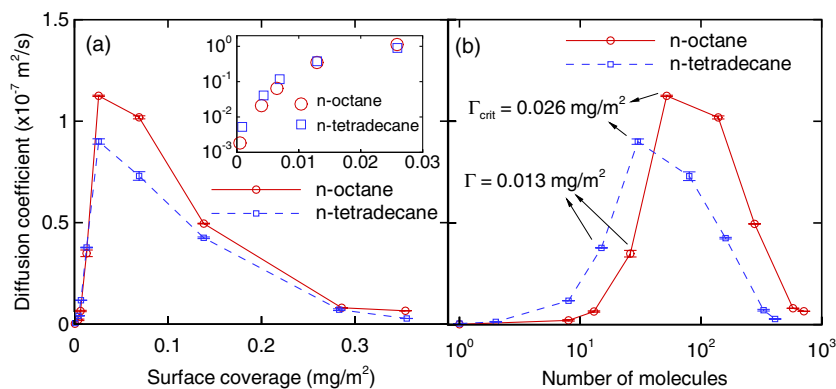


Fig. 2. Variation of the lateral diffusion coefficient with surface coverage: (a) plot based on mass surface coverage (inset) the magnified plot for  $\Gamma < 0.03 \text{ mg/m}^2$ , y-axis is in log-scale and the error-bars are omitted; (b) plot based on the number of molecules per area  $A = 381.38 \text{ nm}^2$ .

from the longest relaxation mode of the chain [18],  $\frac{\langle \theta_{\text{ec}}(t)\theta_{\text{ec}}(0) \rangle}{\theta_{\text{ec}}^2(0)} = \exp\left(-\frac{t}{\tau_R}\right)$ , where  $\theta_{\text{ec}}(t)$  is the angle between the end-to-end vector and a reference axis (e.g. the  $x$ -axis). Since both  $n$ -octane (aspect ratio  $\approx 90$ ) and  $n$ -tetradecane (aspect ratio  $\approx 85$ ) are prolate enough to be considered as rod-like molecules, we expect the scaling relation in Eq. (2) to hold for bulk chains. Using MD simulations for bulk chains, we computed  $(r_{\text{ec}}, \tau_R) = (0.75 \text{ nm}, 16.12 \text{ ps})$  for  $n$ -octane and  $(r_{\text{ec}}, \tau_R) = (1.23 \text{ nm}, 60.5 \text{ ps})$  for  $n$ -tetradecane. Accordingly,  $r_{\text{ec}}^2/\tau_R$  is 0.0432 for  $n$ -octane and 0.0247 for  $n$ -tetradecane and their ratio ( $n$ -octane to  $n$ -tetradecane) is 1.78. This value is quite comparable to the ratio of the diffusion coefficients, 1.84. The length effects ( $r_{\text{ec}}^2$ ) are balanced by  $\tau_R$  and as a result the longer  $n$ -tetradecane moves slower than  $n$ -octane in bulk solutions. In the case of surface diffusion, the molecules are subjected to an additional topological constraint imposed by their interaction with the graphite surface and, hence, their motions are similar to reptation (see Fig. 1). To account for this, we modify Eq. (2) by replacing  $\tau_R$  with the reptation time,  $\tau_{\text{rep}}$ , i.e.,  $D \sim r_{\text{ec}}^2/\tau_{\text{rep}}$ . Considering the simple relation for the Rouse chain,  $\tau_{\text{rep}} = N\tau_R$ , where  $N$  is the number of the segments, and  $r_{\text{ec}}^2 = Nb^2$  for freely jointed chain molecules, where  $b$  is the effective bond length (Kuhn length) [17,18], the scaling law for the diffusion of  $n$ -alkanes on a solid surface for incomplete coverage cases can be written as

$$D \sim \frac{r_{\text{ec}}^2}{N\tau_R}. \quad (3)$$

In our calculations, we observed that while the scaling law given in Eq. (3) can reasonably explain the trend in the diffusion coefficient shown in Fig. 2, a generalized scaling law of the form

$$D \sim \frac{r_{\text{ec}}^2}{N^p\tau_R} \quad (4)$$

with  $p = 1.5$  can better explain the faster diffusion of  $n$ -tetradecane over  $n$ -octane for low surface coverage compared to that of Eq. (3) where  $p = 1.0$ . Physically, Eq. (4) states that the diffusion coefficient of chain molecules on a solid surface depends on molecule–molecule interactions

( $r_{\text{ec}}^2/\tau_R$ ) and molecule–surface interactions ( $1/N^p\tau_R$ ). From Eqs. (2) and (4), it follows that  $D \sim D_{\text{bulk}}/N^p$ .

To demonstrate the scaling law given in Eq. (4), Fig. 3 shows  $r_{\text{ec}}^2/N^{1.5}\tau_R$  and  $1/\tau_R$  of  $n$ -alkanes for various surface coverages. Fig. 3 a and b confirm that  $r_{\text{ec}}^2/N^{1.5}\tau_R$  is a good scaling for the present case, which reveals most of the important features shown in Fig. 2, i.e., the maximum happens at  $\Gamma = \Gamma_{\text{crit}} = 0.026 \text{ mg/m}^2$  and for the high surface coverage ( $\Gamma \geq \Gamma_{\text{crit}}$ )  $n$ -octane moves faster while for the low surface coverage  $n$ -tetradecane moves faster. The simple scaling law of  $D \sim 1/\tau_R$  can also capture the essential features (see Fig. 3c and d), but the difference between the diffusion of  $n$ -octane and  $n$ -tetradecane for low coverage cases is not as significant compared to the MD data. Thus,  $r_{\text{ec}}^2$  and  $N^p$  provide the necessary correction to the simple  $1/\tau_R$  scaling law so that the ratio of the  $n$ -octane to the  $n$ -tetradecane diffusion coefficients is closer to the ratio obtained from MD. Further, the ratio of the  $n$ -octane to the  $n$ -tetradecane diffusion coefficient predicted by Eq. (4) for most of the surface coverages considered here is closer to the corresponding ratio from MD data suggesting that  $p = 1.5$  performs better compared to  $p = 1.0$ . It is, however, important to note that more extensive studies are needed to fully understand the value of  $p$  and the generalized scaling law shown in Eq. (4).

From the above discussion and observations of Figs. 2 and 3, we can conclude that the  $\Lambda$ -shaped anomaly in the diffusion coefficient is mainly dominated by  $\tau_R$  and  $r_{\text{ec}}^2$  and  $N^p$  are the necessary corrections to obtain a proper scaling law. The second question on faster movement of longer  $n$ -tetradecane compared to shorter  $n$ -octane for low surface coverages can be understood by understanding the faster rotational relaxation time of  $n$ -tetradecane compared to  $n$ -octane.

The rotational motion of a molecule can be understood further by considering three interactions: (1) intramolecular, (2) intermolecular, and (3) molecule–surface interactions. Molecule–surface interactions were examined by computing the average distance of  $\text{CH}_3$  and  $\text{CH}_2$  (denoted by  $d_{\text{CH}_3}$  and  $d_{\text{CH}_2}$ ) from the graphite surface. We considered two extreme cases – a single molecule (representing a low surface coverage) over a graphite surface and a fully cov-

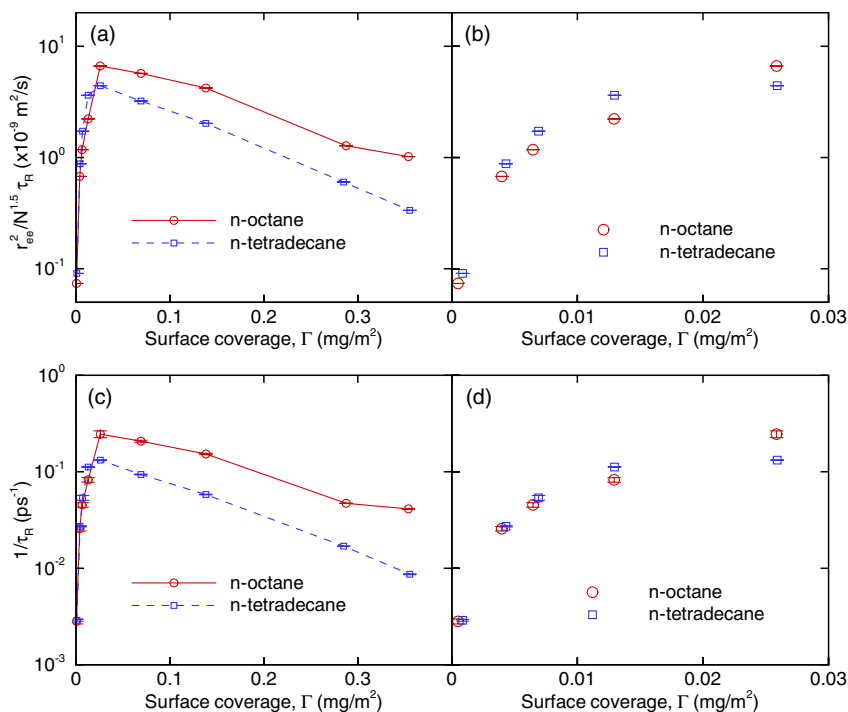


Fig. 3. Variation of  $r_{cc}^2/N^{1.5}\tau_R$  and  $1/\tau_R$  with surface coverage; (a)  $r_{cc}^2/N^{1.5}\tau_R$ ; (b) magnified  $r_{cc}^2/N^{1.5}\tau_R$  for  $\Gamma < 0.03 \text{ mg/m}^2$ ; (c)  $1/\tau_R$ ; (d) magnified  $1/\tau_R$  for  $\Gamma < 0.03 \text{ mg/m}^2$ .

ered graphite surface ( $\Gamma = \Gamma_{\text{full}}$ ). For the single molecule case,  $d_{\text{CH}_3} = 3.840 \text{ \AA}$  and  $d_{\text{CH}_2} = 3.906 \text{ \AA}$  for *n*-octane, and  $d_{\text{CH}_3} = 3.871 \text{ \AA}$  and  $d_{\text{CH}_2} = 3.920 \text{ \AA}$  for *n*-tetradecane, implying that the *n*-octane molecule interacts strongly with the surface compared to the *n*-tetradecane. As a result, the rotation of *n*-octane is slower compared to *n*-tetradecane. For the  $\Gamma = \Gamma_{\text{full}}$  case, *n*-tetradecane ( $d_{\text{CH}_3} = 4.370 \text{ \AA}$ ,  $d_{\text{CH}_2} = 3.590 \text{ \AA}$ ) is closer to the surface compared to the *n*-octane molecule ( $d_{\text{CH}_3} = 5.108 \text{ \AA}$ ,  $d_{\text{CH}_2} = 3.987 \text{ \AA}$ ). Hence, *n*-octane rotates faster compared to *n*-tetradecane. In summary, the molecule–surface interactions explain the fast rotation of *n*-tetradecane for the low coverage case and *n*-octane for the high surface coverage case. The intramolecular (bending, torsion, and Lennard-Jones) and intermolecular (Lennard-Jones) interactions were evaluated together by considering a single molecule in free space for the low coverage limit and a bulk situation for the  $\Gamma = \Gamma_{\text{full}}$  limit. For the single molecule case,  $\tau_R \cong 1600 \text{ ps}$  for *n*-octane and  $\tau_R \cong 1200 \text{ ps}$  for *n*-tetradecane. For the bulk case,  $\tau_R \cong 16.12 \text{ ps}$  for *n*-octane and  $\tau_R \cong 60.5 \text{ ps}$  for *n*-tetradecane. These results suggest that *n*-tetradecane rotates faster for the low coverage limit and *n*-octane rotates faster for the fully covered limit. In summary, both molecule–surface and inter/intra-molecular interactions favor fast rotation of *n*-tetradecane for the low coverage limit and *n*-octane for the high surface coverage limit.

#### 4. Conclusions

To conclude, lateral diffusion of *n*-alkanes on a graphite surface exhibits a  $\Lambda$ -shape anomaly. This is in contrast to

the critical slowing of diffusion (V-shape) observed in carbon nanotubes [19]. Interestingly, *n*-tetradecane moves faster than *n*-octane for low surface coverage while the shorter *n*-octane molecule moves faster in the high surface coverage. The rotational motion of molecules accounting for inter/intramolecular and surface interactions can explain the anomalous diffusion of *n*-alkanes. Finally, we also proposed a scaling relation which can reasonably explain the trend in the diffusion coefficient.

#### Acknowledgements

This research was supported by NSF under Grant Nos. 0120978, 0328162, and 0523435, and by NIH under Grant PHS 2 PN2 EY016570B.

#### References

- [1] B. Bushan, J.N. Israelachvili, U. Landman, *Nature* 374 (1995) 607.
- [2] J. Becker, G. Günther, R. Seemann, H. Mant, K. Jacob, K.R. Mecke, R. Blossey, *Nat. Mater.* 2 (2003) 59.
- [3] S. Granick, S.C. Bae, *J. Polym. Sci., Part B: Polym. Phys.* 44 (44) (2006) 3434.
- [4] S.A. Sukhishvili, Y. Chen, J.D. Müller, E. Gratton, K.S. Schweizer, S. Granick, *Nature* 406 (2000) 146.
- [5] J. Zhao, S. Granick, *J. Am. Chem. Soc.* 126 (2004) 6242.
- [6] J. Zhao, S. Granick, *Macromolecules* 40 (2007) 1243.
- [7] D. Mukherji, M.H. Müser, *Phys. Rev. E* 74 (2006) 010601.
- [8] T.K. Xia, J. Ouyang, M.W. Ribarsky, U. Landman, *Phys. Rev. Lett.* 69 (1992) 1967.
- [9] J.I. Siepmann, S. Karaborni, B. Smit, *Nature* 365 (1993) 330.
- [10] G. Chen, Y. Guo, N. Karasawa, W.A. Goddard III, *Phys. Rev. B* 48 (1993) 13959.
- [11] E. Lindahl, B. Hess, D. van der Spoel, *J. Mol. Model.* 7 (2001) 306.

- [12] B. Hess, H. Bekker, H.J.C. Berendsen, F.G.E.M. Fraaije, *J. Comp. Chem.* 18 (1997) 1463.
- [13] S. Nosé, *Mol. Phys.* 52 (1984) 255.
- [14] W.G. Hoover, *Phys. Rev. A* 31 (1985) 1695.
- [15] P. de Saint Claire, K.C. Hess, W.F. Schneider, W.L. Hase, *J. Chem. Phys.* 106 (1997) 7331.
- [16] M. Doi, S.F. Edwards, *J.C.S. Faraday Trans. II* 74 (1978) 560.
- [17] M. Doi, *Introduction to Polymer Physics*, Clarendon Press, Oxford, 1996.
- [18] M. Rubinstein, R.H. Colby, *Polymer Physics*, Oxford University Press, Oxford, 2003.
- [19] R.J. Mashl, S. Joseph, N.R. Aluru, E. Jakobsson, *Nano Lett.* 3 (2003) 589.
- [20] W. Humphrey, A. Dalke, K. Schulten, *J. Mol. Graph.* 14 (1996) 33.